Article

Ultrafine Aerosol Penetration through Electrostatic Precipitators

Sheng-Hsiu Huang, and Chih-Chieh Chen

Environ. Sci. Technol., **2002**, 36 (21), 4625-4632• DOI: 10.1021/es011157+ • Publication Date (Web): 20 September 2002

Environ. Sci. Technol. **2002**, *36,* 4625−4632

Ultrafine Aerosol Penetration through Electrostatic Precipitators

SHENG-HSIU HUANG AND CHIH-CHIEH CHEN*

Institute of Occupational Medicine and Industrial Hygiene, College of Public Health, National Taiwan University, 1 Jen-Ai Road, Section 1, Taipei, Taiwan

This work measures the penetration of ultrafine particles through a single-stage and a two-stage ESP as a function of particle size. Also studied herein are how parameters including particle size, rate of airflow through the ESP, and voltage of the discharging electrode affect aerosol penetration through the ESP. Monodisperse particles with sizes between 10 and 60 nm were generated as the challenge aerosols to investigate the particle charges given by an ESP. A comparison of experimental and theoretical results confirms that a partial charging regime exists when the particle diameter is several tens of nanometers. Experimental results indicated that aerosol penetration through the single- and two-stage ESPs increased significantly for particles below 20 and 50 nm, respectively. However, the exact regime depends on the parameters including airflow rate, applied voltage, and configuration of the ESP. Phenomena such as ionic flow, particle space charge, and flow turbulence may significantly affect the collection efficiency of an ESP for ultrafine particles. To achieve the same collection efficiency, it is more economical to use single-stage ESPs to collect particles less than 16 nm from the standpoint of energy consumption. However, it is more economical to use two-stage ESPs to collect particles larger than 16 nm.

Introduction

Historically, controlling particulate emissions into the atmosphere has emphasized reducing the mass of the discharged material. However, recent studies have shown that fine particles, defined as those less than 2.5 μm in diameter, have a greater impact on visibility, health, and water droplet nucleation than larger particles. Moreover, the extended time fine particles spend in the atmosphere makes them more difficult to control than larger particles. Accordingly, new particulate matter standards, based on an aerodynamic diameter below 2.5 μm, were proposed (*1*). Although fine particles do not significantly contribute to the mass base of an electrostatic precipitator's (ESP) outlet emission, they may become more important in light of new or future health regulations regarding $PM_{2.5}$ aerosol. Consequently, with the adoption of these new standards, we are interested in the performance of control devices in the fine particle range.

Although it is not clear from the epidemiology standpoint whether it is the mass, number or even the surface area of particles that is the most important determinant of health impact, some toxicological studies showed that particles with diameter less than 100 nm (also referred to as ultrafine particles) exert a much stronger physiological effect than the same mass of coarse particles (*2*, *3*). In theory therefore, if the ultrafine aerosol hypothesis is correct, the use of mass, which is dominated by larger particles, may in some circumstances seriously misrepresent the toxicity of the pollutant. It is thus desirable to investigate the capacities of conventional air pollution control equipments for collecting ultrafine particles.

In many industries, ESPs are widely used as economical and efficient air pollution control devices. Although they often demand the highest capital investment of all comparable methods for removing pollutants from effluent gas streams, the low operating and maintenance costs, the high collection efficiencies, and the ability to withstand severe operating conditions make ESPs ideally suited for application to a variety of industrial pollution problems.

ESPs capture particles by using electrical mechanisms, and thus the efficiency of an ESP depends mainly on its ability to charge particles. There are two principal charging mechanisms: diffusion charging and field charging. Charging of particles takes place when ions bombard the surface of a particle. Although particle charge decreases with particle size, mechanical mobility increases rapidly with decreasing size. Consequently, there is a theoretical minimum collection efficiency in the size range of 0.1−1 μm (*4*). This is a value similar to that observed in the filtration characteristics of mechanical filters (*5*). This U-shape collection efficiency curve has been verified by many experimental studies (*5*−*9*). Although the overall mass collection efficiency of conventional ESPs can easily exceed 99%, the penetration of submicrometer particles can be in tens of percent (*8*, *10*), when calculated in terms of number density rather than mass. Interestingly, the collection efficiency for particles smaller than several tens of nanometers decreased with decreasing particle size (*6*, *7*, *11*). As concluded in many studies, this fact implies the existence of a limited particle charging regime in which a portion of the incoming particles are not charged (*7*, *10*, *11*). There has been considerable interest in determining a mechanism for the charging of ultrafine particles in the past decades. The need to extend the useable range of differential mobility analyzers is the impetus for these studies (*12*−*16*). In this study, the charges of the particles in this regime were also measured in order to investigate the penetration characteristics of partially charged particles through ESPs.

ESPs are configured in several ways. Some of these configurations have been developed for special control, and others have evolved for economic reasons. Although ESPs are operated using the same mechanisms to collect particles, the filtration characteristics of ESPs may differ with different configurations.

To further understand the behavior of ultrafine particles (diameter < 100 nm) in ESPs, a controlled experimental study was conducted. The penetration of ultrafine particles through single- and two-stage ESPs is presented as a function of particle size. The existence of partially charged particles is examined experimentally.

Materials and Methods

Figure 1 schematically depicts the test system. Sucrose was selected as the test material. A constant output atomizer (model 3076, TSI Inc.) was used to generate polydisperse ultrafine challenge aerosol particles. These were then passed through an aerosol neutralizer. The neutralized aerosols were mixed with dried and filtered air to obtain the desired flow rates and to ensure that the aerosol particles were completely

* Corresponding author phone: +886 2 239 38 631; fax: +886 2 232 15 714; e-mail: ccchen@ccms.ntu.edu.tw.

10.1021/es011157+ CCC: $22.00
Published on Web 09/20/2002

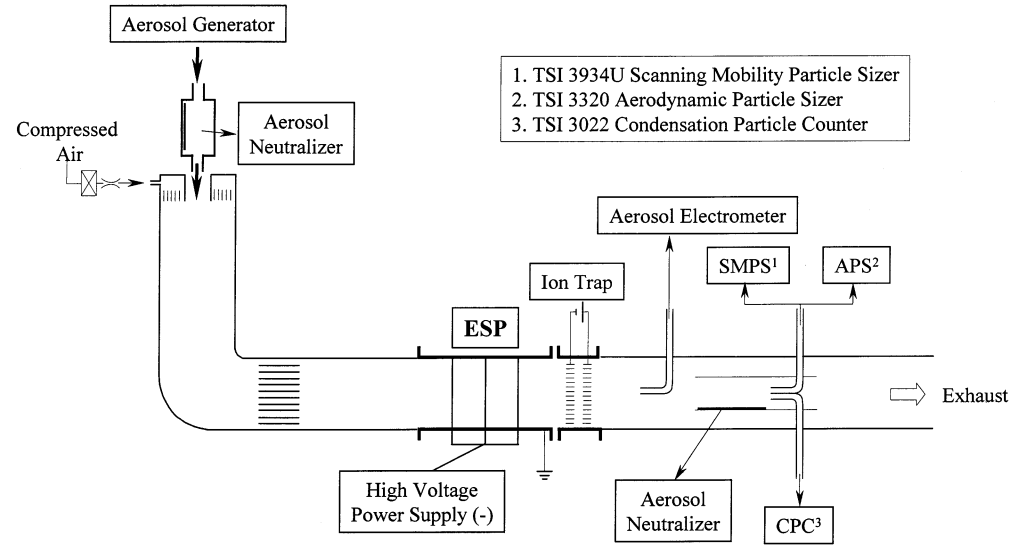

FIGURE 1. Schematic diagram of the experimental setup.

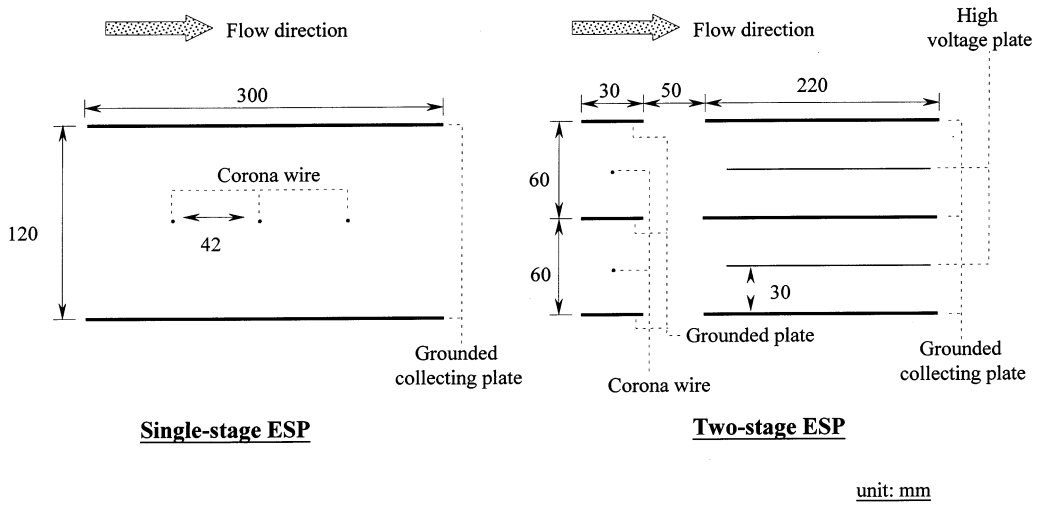

FIGURE 2. Configurations of the single- and the two-stage ESPs (top view).

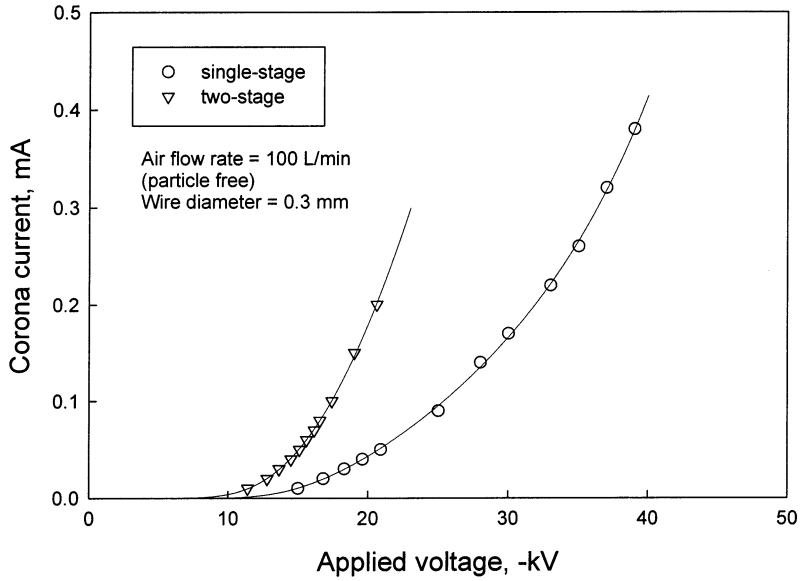

FIGURE 3. Current–voltage (I–V) curves for single- and two-stage ESPs.

dry prior to entering the ESP system. In this work, the airflow rate was 100 L/min (residence time, t, is 1.64 s) unless otherwise specified. The particle number concentration of upstream aerosols was about 1.2×10^5 count/cm^3 with a count median diameter (CMD) of 42 nm and a geometric standard deviation (GSD) of 1.8. An electrospray aerosol generator

TABLE 1. Dimensions and Operating Conditions

		Single-Stage ESP	
radius of wire	0.3 mm	height of ESP	76 mm
no. of wires	3 (series)	wire to wire space	42 mm
length of ESP	300 mm	applied voltage of corona wire	−15.5 to −26 kV
width of ESP	120 mm	airflow rate	50, 100, 150 L/min
		Two-Stage ESP	
charging cell		collecting cell	
radius of wire	0.3 mm	length	200 mm
no. of wires	1	width	30 mm
length	50 mm	height	76 mm
width	60 mm	no. of collecting cell	4 (parallel)
height	76 mm	applied voltage of corona wire	−2 to −14 kV
no. of charging cell	2 (parallel)	airflow rate	100 L/min
		Parallel Plate Ion Trap	
applied voltage	dc 15 V	size of ion trap	$55 \times 55 \times \pi \times 15$ mm^3
distance between two plates	5 mm		

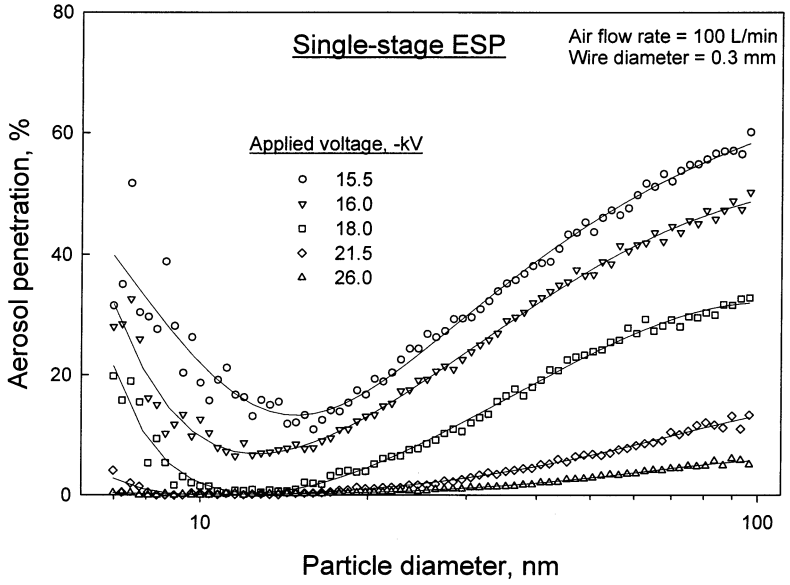

FIGURE 4. Ultrafine aerosol penetration through the single-stage ESP as a function of aerosol size under different applied voltages.

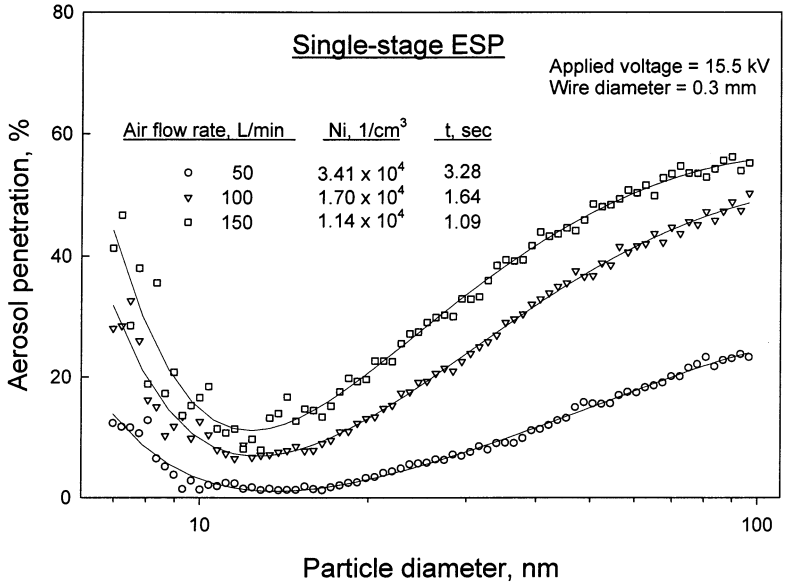

FIGURE 5. Ultrafine aerosol penetration through the single-stage ESP as a function of aerosol size at different testing flow rate.

(model 3480, TSI, Inc.) was used to generate monodisperse ultrafine particles as the challenge aerosol to investigate the ultrafine particle charges given by ESPs. Two types of ESP, a single-stage and a two-stage model, following the conventional wire−plate approach were built and tested in the present study. The physical configurations of these ESPs are

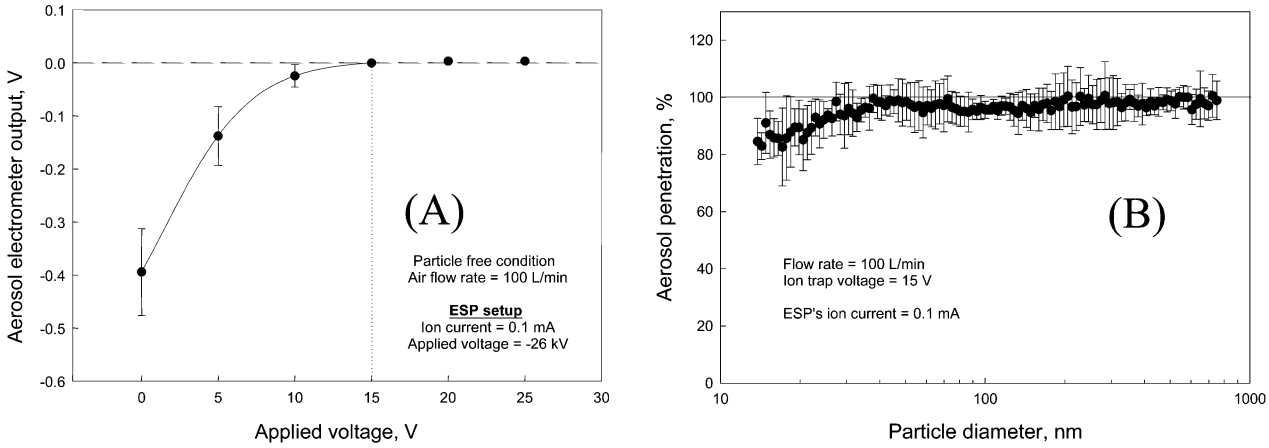

FIGURE 6. Performance characteristic curve of the ion trap.

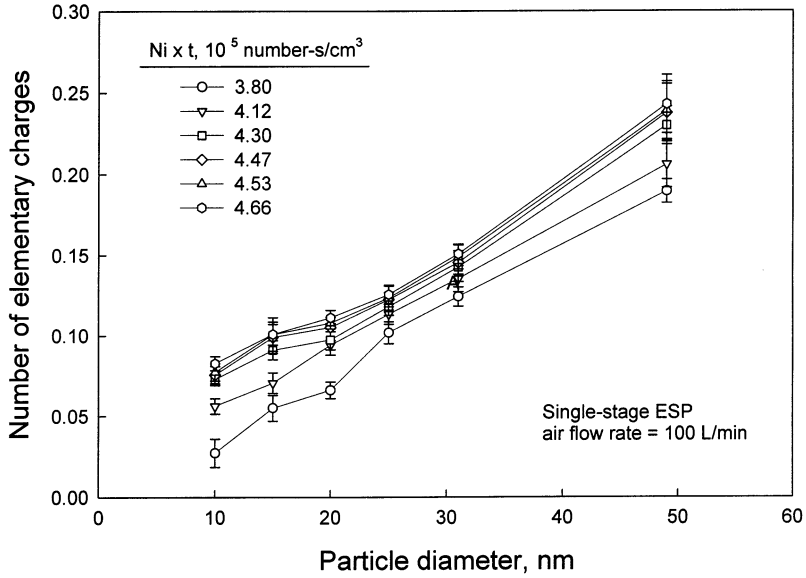

FIGURE 7. Particle charges acquired in the single-stage ESP.

shown in Figure 2. The dimensions and operating conditions are listed in Table 1. Copper wires that are 0.3 mm in diameter were used as discharge electrodes. A high-voltage DC power supplier (model SL50PN300, Spellman High Voltage Electronics Corporation) was used to supply a charging negative voltage (0−30 kV) to the discharged electrodes. The values of the output voltage and current were read directly from the power supply. To avoid the interference of high-mobility negative ions, a small electrical field was applied immediately behind the outlet of the ESPs. A scanning mobility particle sizer (SMPS, model 3934U, TSI Inc.) and an aerodynamic particle sizer (APS, model 3320, TSI Inc.) were used to measure the aerosol concentrations and size distributions. The SMPS measures the particle number concentrations and size distribution in the submicron size range by using the electrical mobility detection technique. The APS, which uses the time-of-flight particle sizing technology, was capable of counting and sizing micrometer-sized particles that generated by an ultrasonic atomizing nozzle (model 8700-120, Sonotek Inc., Highland, NY). Both particle size spectrometers were calibrated using the polystyrene latex, PSL, particles (Duke Scientific Corp.). Particle number concentration data, obtained in the power-on and power-off modes, were used to evaluate the penetration of the aerosol through the ESPs. The total aerosol charge was measured with an aerosol electrometer (model 3068, TSI, Inc.). The average charge in each particle was then determined using the total particle number concentration measured by the condensation particle counter (CPC, model 3022, TSI Inc.). The CPC first grows smaller particles to larger alcohol droplets and then measures the droplet concentrations in an optical chamber. The temperature and relative humidity in the testing chamber were 20−25 °C (room temperature) and 10−15%, respectively.

Results and Discussions

Figure 3 shows the relationship between corona current and applied voltage. Both the single- and two-stage ESPs were examined with clean plates in a particle-free chamber. Using the empirical formulas (*17*, *18*), the corona onset voltage for the single- and two-stage ESPs were calculated to be −10 and −8.7 kV, respectively. The calculated results coincide well with the measured values, as shown in Figure 3. As expected, the corona current increased nonlinearly after the corona onset point as the applied voltage increased.

The experimental results concerning the penetration of aerosol through the ESPs as a function of particle size are shown in Figures 4 and 5 for the single-stage ESP and in Figure 10 for the two-stage ESP. In Figure 4, the aerosol penetration through the ESP was measured under five different applied voltages. A higher applied voltage resulted in lower aerosol penetration because of a higher electrical field strength and corona current. For example, the penetration of the 100-nm particles decreased from 60% to 5% as the applied voltage increased from −15.5 to −26.0 kV. In general, the aerosol penetration decreased with decreasing

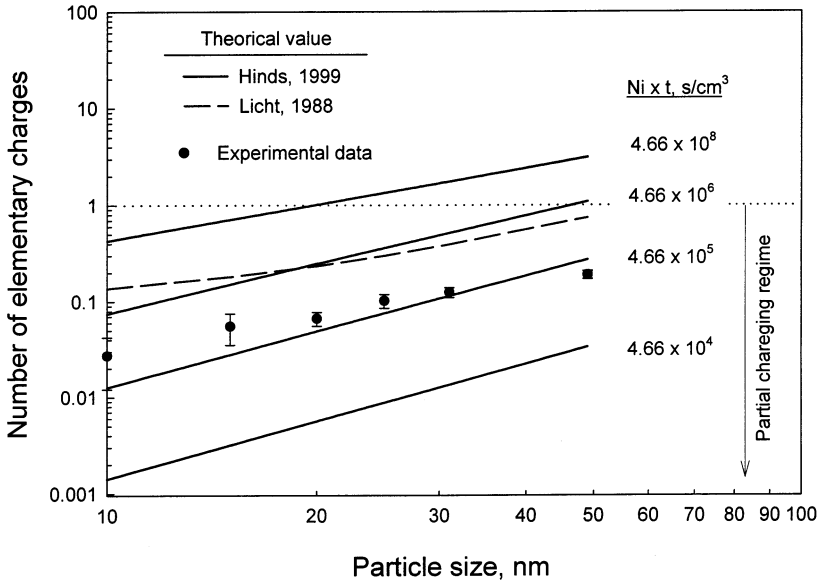

FIGURE 8. Comparison of experimental and theoretical results of the averaged particle charge.

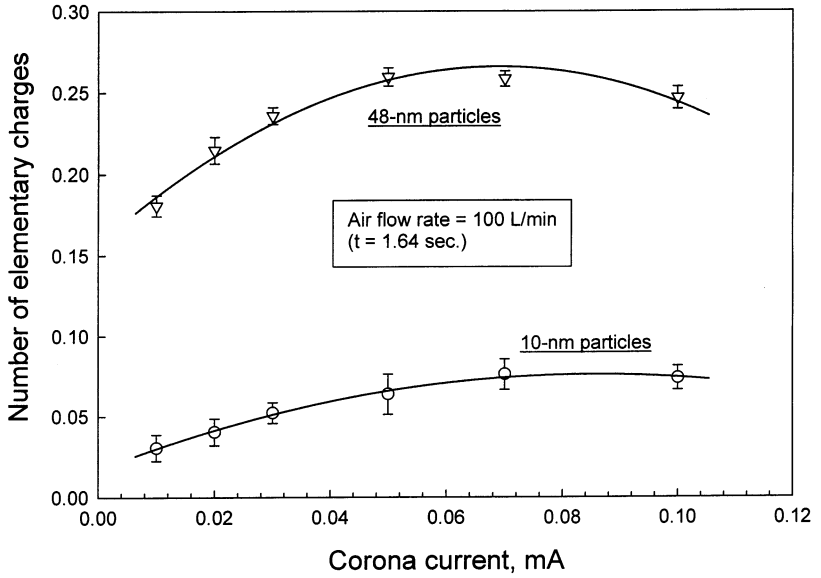

FIGURE 9. Average elementary charge carried by 10- and 48-nm particles under different corona current conditions.

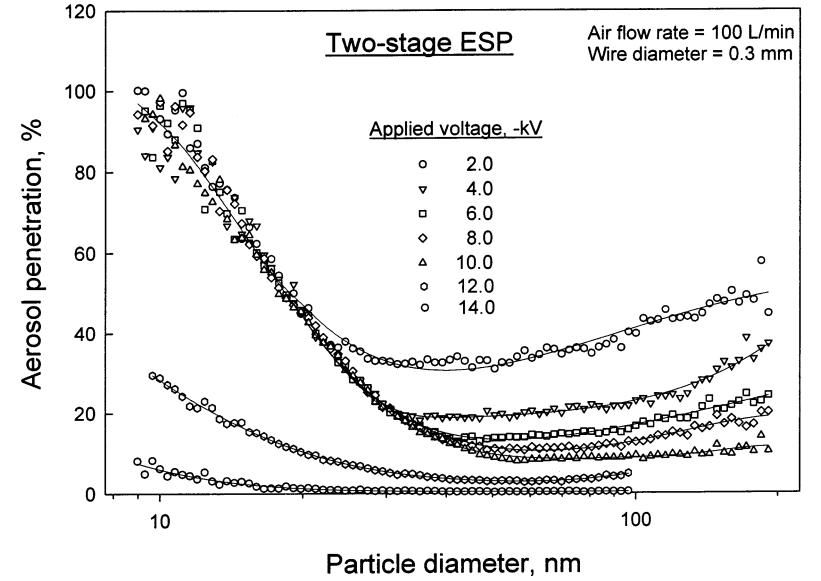

FIGURE 10. Ultrafine aerosol penetration through the two-stage ESP as a function of particle size under different applied voltages.

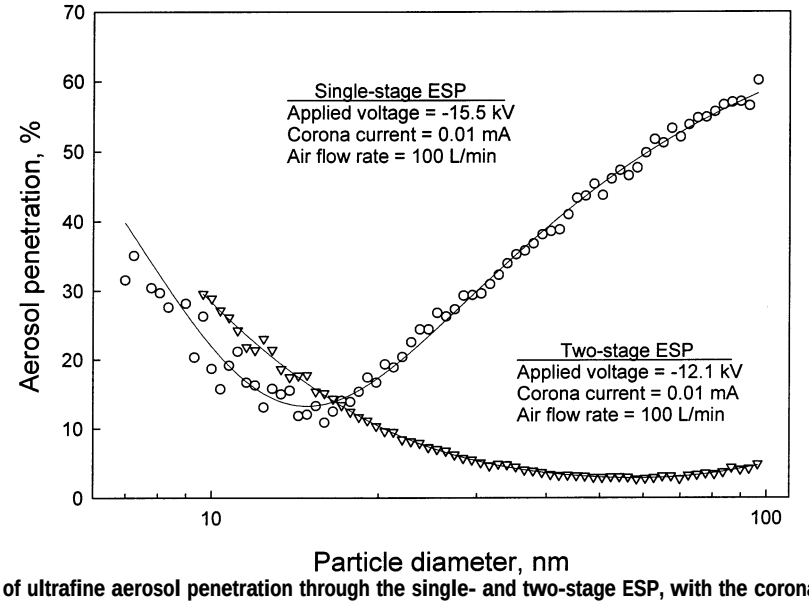

FIGURE 11. Comparison of ultrafine aerosol penetration through the single- and two-stage ESP, with the corona current of 0.01 mA and air flow of 100 L/min.

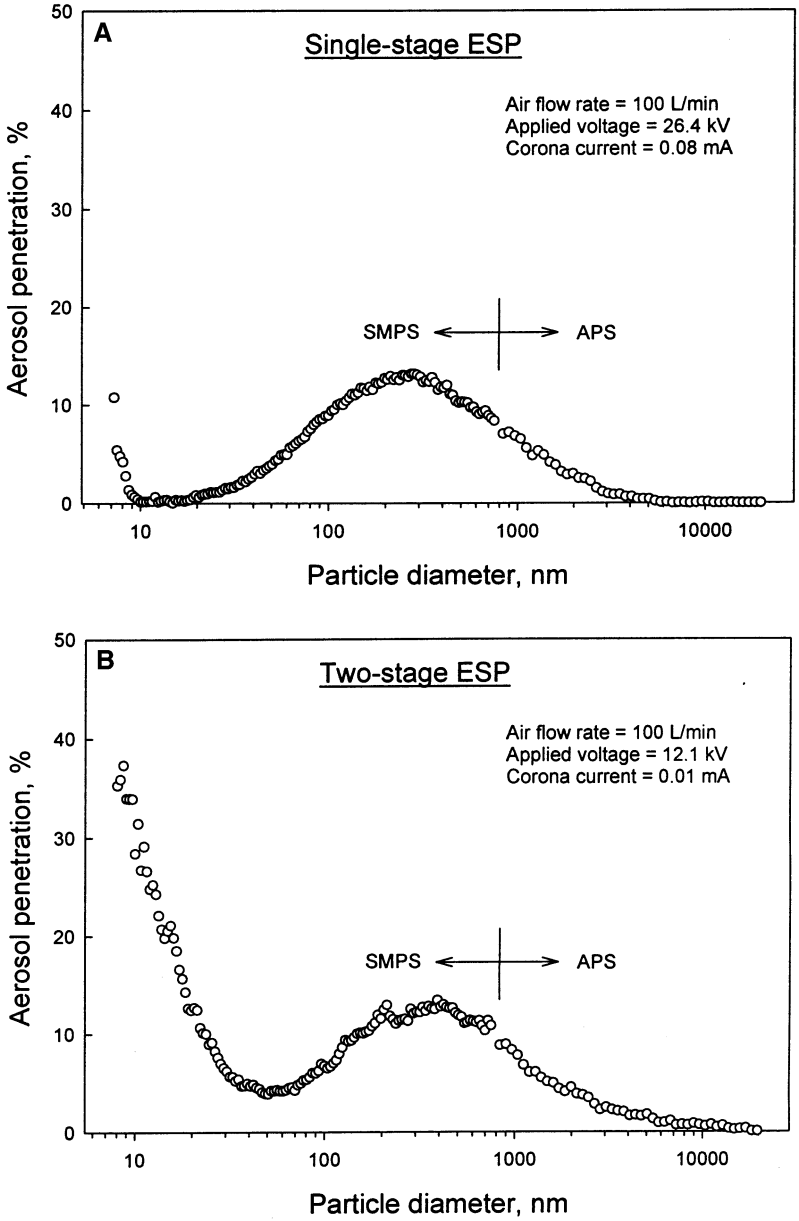

FIGURE 12. Comparison of aerosol penetration patterns of the single- and two-stage ESPs.

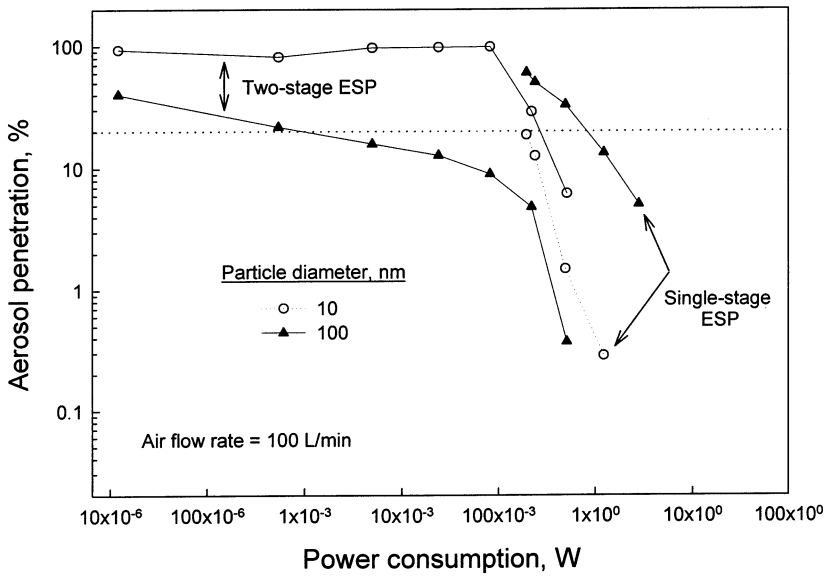

FIGURE 13. Aerosol penetration (diameter, 10 and 100 nm) and power consumption of the single- and two-stage ESPs.

particle size, from 100 nm until it reached a penetration minimum around 15 nm. Then, aerosol penetration increased again with decreasing aerosol size. The increase in aerosol penetration in the ultrafine particle region was also observed by Yoo et al. (*7*) and Zhuang et al. (*10*). These authors have ascribed this phenomenon to the fact that some particles were not charged. In this study, the phenomenon of partial charging was investigated experimentally and theoretically. The results are shown in Figures 7 and 8, respectively.

However, the partial charging effects on the aerosol penetration became less obvious as the applied voltage increased to −26kV. Greater than 99% of particles with a diameter less than 20 nm were collected. This result does not seem to support the concept of partial charging. This is probably due to the following reasons: (i) It has been shown that the electrical potential in the ESP was higher than the applied voltage when the particle space charge density was very high (*19*, *20*). The enhanced electrical field augmented the particle charging and, therefore, the collection efficiency. (ii) The secondary flow caused by the ions that flow from the discharging wire to the grounded electrode is generally known as electric, corona, or ionic wind (*21*). This increased as the flow velocity became smaller, especially when the flow velocity was less than 0.6 m/s (*21*) or when the applied voltage was high. A strong ionic flow may force particles, especially ultrafine ones, to move toward the collecting plates and subsequently be collected. (iii) Turbulent diffusion may also contribute to the high collection efficiency of ultrafine particles in an ESP by increasing the probability of particles collision with collecting surfaces.

Figure 5 shows increasing aerosol penetration with increasing flow rate because of a reduction of residence time in the ESP. For example, when filtration flow increased from 50 L/min ($t = 3.28$ s) to 150 L/min ($t = 1.09$ s), the penetration of 100-nm particles through the ESP increased from 23% to 55%. The increase in aerosol penetration resulting from partial charging of aerosol is also observed in Figure 5.

The aerosol electrometer used an absolute filter to remove the charged particles from the airstream. The readings of the aerosol electrometer could be altered by the existence of free ions if an ion trap was not used. Figure 6A shows the performance of the ion trap for different applied voltages in particle-free condition when the ESP operated at −26 kV (ion current = 0.1 mA). A voltage of +15 V was required to remove free ions when the corona current was 0.1 mA, which was the maximum value used in this study. However, the ion trap was used to remove the excess ions but not the particles. Figure 6B shows the aerosol penetration (through the ion trap) of charged particles (ESP's corona current = 0.1 mA) in the 10−800-nm size range when a +15 V is applied to the ion trap. Almost 100% penetration was obtained down to 30 nm and maintained above 94% and 85% at 25 and 13 nm, respectively.

Figures 7 and 8 show the experimental and theoretical results, respectively, concerning the number of particle charges given by the single-stage ESP. In Figure 7, the values of the product of the ion number concentration (*Ni*) and the charging time (*t*) were changed from 3.8×10^5 to 4.66×10^5 s/cm^3. The graph shows that the particle charge increased with the particle diameter and with the value of *Nit*. By using the particle charging equations of Hinds (*22*), Figure 8 showed theoretical results calculated with different *Nit* values. The measured values were also compared with values calculated using Cochet' charge equation (*23*), which was also used in many studies (*24*, *25*) to predict the performance of an ESP. An average charge of below one elementary charge meant that some particles were uncharged and would not be collected in the ESP. This situation was called partial charging (*7*). The partial charging regime depended on the value of *Nit*. When tested with a larger *Nit*, the upper size limit of the partial charging shifted to a smaller size. In Figure 8, the experimental results closely matched the theoretical prediction of Hinds, although the slopes were slightly different. This difference might be due to the losses of more heavily charged particles in the ESP, especially for larger particles (i.e., the charges of larger particles might be underestimated when compared to the smaller ones). This inference was indirectly supported by the appearance of maximum values of curves shown in Figure 9, illustrating the average elementary charge carried by 10- and 48-nm particles under different corona current conditions. Since particle loss can increase with *Nit* faster than the acquisition of charge and the more heavily charged particles are preferentially removed, it is possible for there to be a maximum in the curve. This was observed experimentally in two studies (*14*, *15*) as well. If the particle loss in the ESP had been neglected in the model calculations, then these curves would have been monotonically increasing (*15*). Furthermore, the experimental data have slope that are strikingly close to that predicted by Licht, although there seems to be some systematic lowering from this theoretical line. If an adjustment of particle loss were made, it would be tempting to say that the experimental

data might be more closely aligned with the theoretical data of Licht than the theoretical data of Hinds. Clearly, this area needs further studies.

Aerosol penetration through the two-stage ESP at different applied voltages was also investigated. The results are shown in Figure 10. As expected, the aerosol penetration through the ESP decreased as the applied voltage increased. When the applied voltage was below −10 kV, however, the collection efficiency of particles with a diameter of less than 20 nm decreased significantly. This was because the applied voltage was lower than the onset voltage of the two-stage ESP shown in Figure 3. The partial charging effect could also be observed with the two-stage ESP. Figure 10 shows that aerosol penetration decreased as aerosol size decreased from 200 to 50 nm. At this point, aerosol penetration started to increase. This concurs with the results of Yoo et al. (*7*).

Figure 11 shows the difference in aerosol penetration between single- and two-stage ESPs for a given corona current (0.01 mA) and airflow rate (100 L/min) ($t = 1.64$ s). The two-stage ESP was obviously more efficient when used to collect particles with diameters more than 20 nm. However, the collection efficiency of the two-stage ESP for particles smaller than 20 nm in diameter was slightly lower than that of the single-stage ESP. The difference in the aerosol penetration characteristics was likely due to different collection processes such as turbulent diffusion, since the values of *Nit* were the same for both ESPs. Therefore, a higher electrical field in the collecting cell of the ESP would improve particle collection efficiency, especially for particles larger than 20 nm. Moreover, ESPs with different configurations might also affect the penetration minimum

Figure 12 shows the filtration characteristics of single- and two-stage ESPs for 10 nm−10 μm particles. The aerosol penetration data points for sizes above 0.8 μm were measured using an aerodynamic particle sizer (APS, model 3320, TSI Inc.), and were described in detail elsewhere (*26*). Figure 12 shows that aerosol penetration curves through both ESPs for particle sizes above 50 nm were almost identical. However, the two-stage ESP exhibited less efficiency than the single-stage ESP for particles smaller than 50 nm. Figure 12 also shows that the collection minimum of the two-stage ESP no longer fell within the 0.2−0.5 μm range (*4*, *9*, *23*). This phenomenon needs to be considered when developing the performance testing requirements for ESPs. Notably, both the applied voltages and the corona currents of the ESPs were different in this case. Therefore, an index "power consumption", which was the product of voltage and current, was used to objectively compare the performance of these two ESPs. Figure 13 shows the relationship between the power consumption and the aerosol penetration of these two ESPs, when used to collect 10- and 100-nm particles. The single-stage ESP, when used as an air cleaning device, consumed 0.2 W to collect 80% of the 10-nm particles and 1 W to collect the same percentage of the 100-nm particles. The two-stage ESP consumed 0.35 and 0.001 W to collect 80% of the 10- and 100-nm particles, respectively. Therefore, to achieve the same collection efficiency, it is more economical to use single-stage ESPs to collect particles smaller than 16 nm. However, it was more economical to use two-stage ESPs to collect particles larger than 16 nm.

Acknowledgments

The authors thank the National Science Council of Taiwan for financially supporting this research under Contract NSC 91-2621-Z-002-024.

Literature Cited

(1) U.S. EPA. *National Air Quality and Emissions Trends Report*, 1996; http://www.epa.gov/oar/aqtrnd96/toc.html.
(2) Oberdorster, G.; Ferin, J.; Gelein, R.; Soderholm, S. C.; Finkelstein, J. *Environ. Health Perspect.* **1992**, *97*, 193−199.
(3) Donaldson, K.; Li, X. Y.; MacNee, W. *J. Aerosol Sci.* **1998**, *29*, 553−560.
(4) Hinds, W. C. *Aerosol Technology: Electrical Properties*; John Wiley and Sons: New York, 1982; pp 297, 305.
(5) Chen, C. C.; Huang, S. H. *Am. Ind. Hyg. Assoc. J.* **1998**, *59* (4), 227−233.
(6) McCian, J. D.; Gooch, J. P.; Smith, W. B. *J. Air Pollut. Control Assoc.* **1975**, *25* (2), 117−121.
(7) Yoo, K. H.; Lee, J. S.; Oh, M. D. *Aerosol Sci. Technol.* **1997**, *27*, 308−323.
(8) Ylätalo, S. I.; Hautanen, J. *Aerosol Sci. Technol.* **1998**, *29* (1), 17−30.
(9) Chang, C. L.; Bai, H. *J. Aerosol Sci.* **1999**, *30* (3), 325−340.
(10) Zhuang, Y.; Kim, Y. J.; Lee, T. G.; Biswas, P. *J. Electrost.* **2000**, *48*, 245−260.
(11) Hanley, J. T.; Smith, D. D.; Lawless, P. A.; Ensor, D. S.; Sparks, L. E. *Proceedings of the Fifth International Conference on Indoor Air Quality and Climate*, Toronto, Canada, July 29−August 3, 1990; pp 187−192.
(12) Adachi, M.; Kousaka, Y.; Okuyama, K. *J. Aerosol Sci.* **1985**, *16* (2), 109−123.
(13) Davison, S. W.; Hwang, S. Y.; Gentry, J. M. *Langmuir* **1985**, *1*, 150−158.
(14) Hwang, S. Y.; Gentry, J. W.; Davison, S. W. *J. Aerosol Sci.* **1986**, *17* (2), 117−127.
(15) Davison, S. W.; Yu, P. Y.; Hwang, S. Y.; Gentry, J. W. *J. Aerosol Sci.* **1986**, *17* (3), 481−483.
(16) Chen, D. R.; Pui, D. Y. H. *J. Nanopart. Res.* **1999**, *1*, 115−126.
(17) Flagan, R. C.; Seinfeld, J. H. *Fundamentals of Air Pollution Engineering*; Prentice-Hall: Englewood Cliffs, NJ, 1988.
(18) Anthony, J. B.; Wayne, T. D. *Air Pollution Engineering Manual/ Air & Waste Management Association*; Van Nostrand Reinhold: New York, 1992.
(19) Bohm, J. *Electrostatic Precipitators*; Elsevier: New York, 1982.
(20) Park, S. J.; Kim, S. S. *J. Electrost.* **1998**, *45*, 121−138.
(21) Liang, W. J.; Lin, T. H. *Aerosol Sci. Technol.* **1994**, *20*, 330−344.
(22) Hinds, W. C. *Aerosol Technology: Electrical Properties*; John Wiley and Sons: New York, 1999; p 325.
(23) Litch, W. *Air Pollution Control Engineering*; Marcel Dekker: New York, 1988.
(24) Bai, H.; Lu, C.; Chang, C. L. *J. Air Waste Manage. Assoc.* **1995**, *45*, 908−916.
(25) Lu, C.; Huang, H. *J. Aerosol Sci.* **1998**, *29* (3), 295−308.
(26) Huang, S. H.; Chen, C. C. *Aerosol Sci. Technol.* **2001**, *35*, 792−804.

Received for review July 23, 2001. Revised manuscript received June 26, 2002. Accepted July 24, 2002.

ES011157+